HHS Public Access

Author manuscript

Nanomedicine. Author manuscript; available in PMC 2017 October 01.

Published in final edited form as:

Nanomedicine. 2016 October ; 12(7): 1833–1842. doi:10.1016/j.nano.2016.03.005.

Targeted drug delivery to ischemic stroke via chlorotoxin-anchored, lexiscan-loaded nanoparticles

Liang Han, PhD[a,b], **Qiang Cai, MD**[a,c], **Daofeng Tian, MD**[a,c], **Derek K. Kong**[a], **Xingchun Gou, PhD**[a,d], **Zeming Chen**[a], **Stephen M. Strittmatter, MD, PhD**[e], **Zuoheng Wang**[f], **Kevin N. Sheth, MD**[a,e], and **Jiangbing Zhou, PhD**[a,g,*]

[a]Department of Neurosurgery, Yale University, New Haven, CT 06510, USA

[b]School of Life Science and Technology, Harbin Institute of Technology, Harbin 150080, China

[c]Department of Neurosurgery, Renmin Hospital of Wuhan University, Wuhan 430060, China

[d]The laboratory of Cell Biology and Translational Medicine, Xi'an Medical University, Xi'an 710021, China

[e]Department of Neurology, Yale University, New Haven, CT 06510, USA

[f]Division of Biostatistics, School of Public Health, Yale University, New Haven, CT 06510, USA

[g]Department of Biomedical Engineering, Yale University, New Haven, CT 06511, USA

Abstract

Ischemic stroke is a leading cause of disability and death worldwide. Current drug treatment for stroke remains inadequate due to the existence of the blood-brain barrier. We proposed an innovative nanotechnology-based autocatalytic targeting approach, in which the blood-brain barrier modulator lexiscan is encapsulated in nanoparticles to enhance blood-brain barrier permeability and autocatalytically augment the brain stroke-targeting delivery efficiency of chlorotoxin-anchored nanoparticles. The nanoparticles efficiently and specifically accumulated in the brain ischemic microenvironment and the targeting efficiency autocatalytically increased with subsequent administrations. When Nogo-66 receptor antagonist peptide NEP1-40, a potential therapeutic agent for ischemic stroke, was loaded, nanoparticles significantly reduced infarct volumes and enhanced survival. Our findings suggest that the autocatalytic targeting approach is a promising strategy for drug delivery to the ischemic microenvironment inside the brain. Nanoparticles developed in this study may serve as a new approach for the clinical management of stroke.

[*]**To whom correspondence should be addressed**, Jiangbing Zhou, Department of Neurosurgery, Yale University, 333 Cedar Street, FMB410, New Haven, CT 06510, USA. Tel: +1(203)785-5327. Fax: +1(203)737-2159. jiangbing.zhou@yale.edu.

Conflict of Interest

S.M.S. is a co-founder of Axerion Therapeutics seeking to develop the Nogo-NogoReceptor-based medicines for Neural Repair, and prion protein-based medicines for Alzheimer disease.

Graphical Abstract

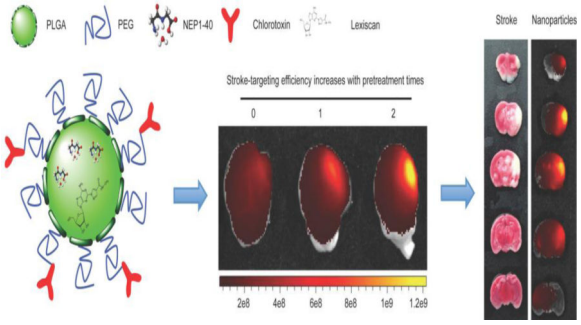

Keywords

Stroke; Blood-brain barrier; Autocatalytic targeting; Lexiscan; Chlorotoxin; Nanoparticles

Background

Ischemic stroke is a leading cause of adult disability worldwide and the fifth most common cause of death in the United States.[1] Current treatment modalities for stroke are inadequate. Intravenous administration of tissue-type plasminogen activator (tPA) within 3 hours of symptom onset is the only FDA-approved pharmacotherapy.[2] However, with such a narrow therapeutic window, it is estimated that only 7% of patients are eligible for tPA treatment.[3] Moreover, accumulating data suggests that reperfusion is not effective,[4-6] but harmful to patients with large infarcts,[7] which occurs in 10-12% of stroke patients.[8] Thus, improved treatment of ischemic stroke requires the development of novel pharmacological approaches.

One of the major challenges for the development of effective treatment for stroke is the lack of approaches for efficient delivery of medicines to the brain, because the brain is protected by the restrictive blood-brain barrier (BBB).[9,10] The BBB is a vital element in regulation of the constancy of the internal environment of the brain, but it also largely hinders the delivery of most therapeutic agents to the brain.[11,12] The BBB may be partially disrupted in later stages following stroke, as evident in 33% of ischemic human patients.[13,14] The mean time from onset of ischemia to the observation of BBB disruption is 4-5 hours in experimental rats[15,16] and 12.9 hours in humans.[13,14] However, the BBB remains intact at least in the initial few hours following the onset of cerebral ischemia, the time that is considered the most critical portion of the therapeutic window.[17] Furthermore, even in brains that experience partial BBB disruption, the degree of leakage may not be adequate for delivery of pharmacologically significant quantities of medication for effective stroke treatment. To overcome the BBB, nanotechnology by using nanoparticles (NPs) is promising, as NPs can be engineered to cross the BBB by exploiting receptor-mediated or adsorptive-mediated transcytosis pathways via surface-conjugation of ligands or display of positive charge.[18-20] Nonetheless, existing engineering approaches typically enhance the delivery of NPs to the brain by less than 5 fold and thus are likely insufficient for systemic treatment of ischemic stroke.[19,21,22] Novel strategies with enhanced delivery efficiency are needed.

In this study, we proposed an innovative approach through the combination of the traditional targeted delivery with a secondary, novel autocatalysis mechanism, for systemic drug delivery to stroke. The traditional targeted delivery, which is achieved using ligands that have high affinity for the ischemic microenvironment, allow a small fraction of NPs to enter the ischemic region of the brain. Immediately after this, NPs will locally release BBB modulators, which in turn transiently enhance BBB permeability to allow additional NPs to enter the same region. Through this secondary autocatalysis mechanism, the delivery procedure creates a positive feedback loop. As a result, the efficiency of NP accumulation in the ischemic region of the brain autocatalytically increases with time and subsequent administrations. We tested the proposed approach by synthesizing NPs using poly(lactic-*co*-glycolic acid) (PLGA), a polymer known to have excellent biocompatibility and biodegradability. PLGA NPs were further engineered through surface display of chlorotoxin (CTX) as a targeting ligand and internal encapsulation of lexiscan (LEX) as the BBB modulator. CTX is a 36-amino acid peptide with high specificity and affinity with matrix metalloproteinase 2 (MMP-2),[23] which is up-regulated in the ischemic microenvironment in the brain.[24-26] LEX, a small molecule drug approved by the FDA for myocardial perfusion imaging, was recently shown to transiently enhance BBB permeability and enhance the drug delivery to the brain.[27,28] Our results suggested that the resulting NPs, designated PLGA-CTX/LEX NPs, allowed for targeted drug delivery to the ischemic microenvironment in the brain with high efficiency. When Nogo-66 receptor antagonist peptide (NEP1-40), a 40-amino acid peptide known to be effective in stroke, was encapsulated in our NPs, PLGA-CTX/LEX NPs significantly reduced infarct volumes, improved neurologic outcomes, and enhanced the survival of stroke mice. Our study reveals a novel approach for drug delivery to the ischemic microenvironment in the brain, which may have a significant impact on clinical management of ischemic stroke.

Methods

Synthesis of PLGA-PLL

Synthesis of PLGA-PLL was accomplished via coupling using dicyclohexyl carbodiimide as previously reported.[29-31] In a typical reaction, PLGA (3 g, 50:50 PLGA Acid End Group; i.v. ~0.67 dL/g; Absorbable Polymers: Pelham, AL) and 200 mg poly(ε-carbobenzoxyl-L-lysine) (PLL) in 5 M excess (1000-4000 MW) were dissolved in 6 mL dimethlyformamide in a dry round-bottom flask under argon. Dicyclohexyl carbodiimide (58 mg) and 0.31 mg dimethylaminopyridine were dissolved in 2 mL dimethlyformamide under argon, then added to the polymer solution and allowed to stir for 48 h. The reacted solution was diluted by the addition of chloroform and precipitated in methanol. The dried polymer was then re-dissolved in chloroform, precipitated in ether, and dried under vacuum for 24 h. Unconjugated PLL was removed during the precipitation and subsequent washes. Dried protected product was placed in a round bottom flask, purged with argon, and dissolved in 10 mL hydrogen bromide, 30% wt in acetic acid and allowed to stir for 90 min for deprotection. The polymer was precipitated in ether and washed until the product changed from a yellow to an off-white appearance. The product was then dissolved in chloroform and precipitated in ether. The polymer was vacuum dried for 24 h to remove all traces of ether. Samples before and after deprotection were collected to confirm modification of the polymer

and subsequent removal of protecting carbobenzoxyl groups. The samples were dissolved in trifluoroethanol and evaluated from 200 to 350 nm using spectroscopy (Cary 50 Bio UV-Vis Spectrophotometer, Varian, Palo Alto, CA).

Synthesis of NPs

NPs loaded with NEP1-40 were synthesized through the double-emulsion solvent evaporation technique. In a typical synthesis, 2.5 mg LEX (Toronto Research Chemicals) in 100 μL dimethyl sulfoxide and 5 mg NEP1-40 (provided by Dr. Stephen M. Strittmatter at Yale) in 200 μL water were added dropwise to 100 mg PLGA-PLL in 2 mL ethyl ether under vortex, respectively. This mixture was sonicated to form a water/oil emulsion (1st emulation). The water/oil emulsion was then added dropwise to 4 mL 2.5% polyvinyl alcohol (PVA, 87-90% hydrolyzed, average molecular weight 30,000-70,000) under vortex and sonicated to form a water/oil/water emulsion (2nd emulation). The double emulsion was poured into a beaker containing 0.3% PVA and stirred for 3 hours. NPs were collected by centrifugation at 20000 rpm for 30 min. The precipitate was suspended in PBS and reacted with 24 mg a-Malemidyl-u-N-hydroxysuccinimidyl polyethyleneglycol, MW 5000 (NHS-PEG-MAL, Jenkem Technology, Beijing, China) for 1 h at room temperature. NPs were collected and excess NHS-PEG-MAL removed by centrifugation at 20000 rpm for 30 min. The precipitate was suspended in PBS and reacted first with 32 μg thiolated CTX (Alamone Labs, Jerusalem, Israel) for 1 h at room temperature and then with excess methoxyl PEG thiol (mPEG-SH, MW350) for 1 h at room temperature. The unreacted CTX and mPEG-SH were removed by centrifugation at 20000 rpm for 30 min, resulting PLGA-CTX/LEX NPs. The precipitate was suspended in H_2O and lyophilized for storage and characterization. NPs without encapsulation of LEX during 1st emulsion were named PLGA-CTX NPs. NPs with direct conjugation with mPEG-SH other than CTX were named PLGA NPs or PLGA-LEX NPs depending on the encapsulation of LEX. The amount of NEP1-40 loaded into the NPs in terms of drug loading (equation [1]) was determined by using FITC-labeled NEP1-40 for synthesizing NPs and dissolving 0.5 mg NPs in 1 mL of dimethyl sulfoxide and measurement by microplate reader (Synergy 2, Bioteck, USA) at an excitation wavelength of 494 nm and an emission wavelength of 518 nm.

For synthesis of IR780-loaded NPs, 1 mg IR780 in 100-μL dimethlyformamide, 5 mg LEX in 100-μL dimethyl sulfoxide, and 200-μL water were added dropwise to 100 mg PLGA-PLL in 2 mL ethyl ether under vortex, respectively, to create the water/oil emulsion. Remaining procedures are similar to those mentioned above.

$$\text{Drug loading}\,(\%) = \frac{\text{Determined amount of NEP1-40 in nanoparticles}}{\text{Weight of nanoparicle}} \times 100\% \quad (1)$$

Scanning electron microscopy (SEM)

The morphology of NPs was characterized by SEM. Briefly, dry NPs were mounted on carbon tape and sputter-coated with gold in an argon atmosphere using a sputter current of 40 mA (Dynavac Mini Coater, Dynavac, USA). SEM analysis was carried out with a Philips XL30 SEM using a LaB electron gun with an accelerating voltage of 3 kV.

Particle size analysis and zeta potential

The hydrodynamic diameter of NPs was measured using dynamic light scattering. A transparent cuvette was filled with 0.25 mg mL^{-1} NPs in HPLC-grade water. The capped cuvette was placed in a Zetasizer (Malvern) and dynamic light scattering data was read. Zeta potential was also measured using the Zetasizer.

Animals

Male C57BL/6 mice (Charles River Laboratories, Willimantic, CT, USA), 18-22 gram each, were given free access to food and water before the experiment. All animal experiments were approved by the Yale University Institutional Animal Care and Utilization Committee.

Middle cerebral artery occlusion (MACO)

MCAO models were generated according to methods that we recently reported.[32] Briefly, the animals were anesthetized with 5% isoflurane (Aerrane, Baxter, Deerfield, IL) in $30\%O_2/70\%N_2O$ using a Tabletop Anesthesia system (Harvard Apparatus, USA) and then isoflurane was maintained at 1.5%. Body temperature of the mice was maintained during surgery with a heating pad. Mice were placed in the supine position. Fur on the neck region was shaved. The surgical site was disinfected with a Povidone-iodine solution. A 1 cm long midline neck incision was made under a dissecting microscope (Leica A60). Blunt dissection was performed to expose the right common carotid artery (CCA), external carotid artery (ECA), and internal carotid artery (ICA), while preserving the vagus nerve. The CCA was temporarily occluded using 6-0 silk suture and then the bifurcation CCA was isolated. We dissected the ECA further distally, coagulated the ECA and its superior thyroid artery (STA) and occipital artery (OA) using electrocautery, cut the ECA, OA, and STA at the cauterized segment. Two sutures were placed around the ECA stump, one was permanent knot close to the cauterized segment and the other one was temporary knot that was close to the bifurcation. We dissected the ICA and then clipped it with a microvascular clip. Then a small hole in the ECA between the permanent and temporary sutures was made using Vanes-style spring scissors. A 6-0 silicon-coated monofilament suture (Ducal Corporation) was introduced into the ECA. The temporary knot was tightened to prevent bleeding and the microvascular clip on ICA was removed. The monofilament was gently advanced from the lumen of the ECA into the ICA a distance of 8-10 mm beyond the bifurcation to occlude the origin of middle cerebral artery, or until the monofilament could not be further advanced. The occlusion lasted 60 min and the monofilament was withdrawn to allow for reperfusion. The suture on the ECA was permanently tied off and the temporary suture on the CCA was removed to allow blood recirculation. Blood vessel occlusion was further confirmed by measuring cerebral blood flow using a Doppler blood flowmeter (AD Instruments Inc., Colorado Springs, CO, USA) for the duration of the surgery.

Measurement of cerebral blood flow

To determine cerebral blood flow, animals were placed in the supine position, with the head immobilized in a stereotactic frame (Model 900 Small Animal Stereotactic; David Kopf Instruments, Tujunga, CA, USA). A burr hole (1.5 mm diameter) was drilled into the skull using a surgical bone drill system (Microtorque II; Harvard Apparatus, Holliston, MA,

USA) 5–6 mm lateral and 1–2 mm posterior to the bregma, without injury to the dura mater. The laser Doppler flow probe (Standard Pencil Probe, MNP 100XP; AD Instruments, Inc.) was carefully positioned at the craniotomy site using a three-way micromanipulator (Narishige International, Inc., East Meadow, NY, USA). The above procedure was carried out prior to blood vessel occlusion. Cerebral blood flow was continuously monitored (2-Hz sampling rate) from before the onset of ischemia until 5 min after reperfusion. Middle cerebral artery occlusion was confirmed by reduction by over 85% in the local cerebral blood flow from the baseline value. One hour after ischemia, the intraluminal filament was withdrawn to allow for reperfusion, which was confirmed by restoration of the local cerebral blood flow to baseline. The incision was sutured, and animals were allowed to recover, during which time their bodies were kept warm with a heating pad.

Fluorescent imaging of NPs

Immediately after the onset of reperfusion, IR780-loaded NPs with and without modifications were injected intravenously through the tail vein typically at 2 mg NPs/mouse. Three mice were included in each group. Considering that there were slight variances in IR780 loading efficiency among different batches of IR780-loaded NPs, the dose was adjusted according to the fluorescence intensity to ensure that each mouse received the same amount of IR780. Twenty-four hours post-operatively, mice were anesthetized to shave their hair and imaged using an IVIS imaging system (Caliper, CA). Then, mice were sacrificed and the brains were excised for further imaging. Fluorescence intensity in each brain was quantified using Living Image 3.0 (Caliper, CA).

Evaluation of autocatalytic delivery

Mice with successful MCAO surgeries were randomly divided into three groups, with each group containing three mice. To enable autocatalysis, mice in the first group received two pre-treatments of unlabeled PLGA-CTX/LEX NPs, with one immediately after MCAO and another one at 24 hours after MCAO, and then one last treatment with IR780-loaded PLGA-CTX/LEX NPs at 48 hours after MCAO. The second group received one single pre-treatment with unlabeled PLGA-CTX/LEX NPs at 24 hours after MCAO, and then a treatment with IR780-loaded PLGA-CTX/LEX NPs at 48 hours after MCAO. The third group received a treatment with IR780-loaded PLGA-CTX/LEX NPs at 48 hours after MCAO without pre-treatments. Twenty-four hours after treatment with IR780-loaded PLGA-CTX/LEX NPs, mice and excised brains were imaged using an IVIS system as described above. For mice in the first group, other major organs were also imaged. The brains isolated from mice in this group were further sliced coronally and stained with 2,3,5-triphenyltetrazolium chloride (TTC) by incubating the brain sections with 2% TTC solution for 20 min at 37 °C. The images for the TTC staining and the IR780 signal were captured with a camera and an IVIS imaging system, respectively.

Evaluation of therapeutic benefits

Mice were treated with NEP1-40-loaded NPs (n = 17) three times at 0, 24 and 48 hours after surgery. Saline (n = 15), free NEP1-40 (n = 6), and blank NPs (n = 15) were used as controls. The dose of NEP1-40 was 22 μg per mouse for both the NEP1-40-loaded NP group and free NEP1-40 group. Mice were monitored for survival until 14 days after surgery or

until one of the following criteria for euthanasia was met: (1) the mouse's body weight dropped below 15% of its initial weight, and (2) the mouse became lethargic or sick and unable to feed.

Separate groups of mice (n = 6 for each group) were prepared and treated for the evaluation of infarct size. The impact of treatments on infarct size was evaluated at 72 hours after surgery, when mice were sacrificed and the brains were excised, sectioned, and stained with TTC. The size of infarcts was measured using ImageJ and expressed as the percentage of total area.

$$\text{Percentage of infarct area}\,(\%) = \sum \text{infarct area} / \sum \text{total area}$$

Neurologic outcome of each mouse was assessed by a standard behavioral test 24 hours after the last treatment,[33,34] and were scored as follows: 1, normal motor function; 2, flexion of torso and contralateral forelimb when animal was lifted by the tail; 3, hemiparalysis resulting in circling to the contralateral side when held by tail on flat surface, but normal posture at rest; 4, leaning to the contralateral side at rest; 5, no spontaneous motor activity. The number of mice in groups receiving treatment with NEP1-40-loaded NPs, blank NPs, and free NEP was 12, 12, and 6, respectively.

Therapeutic evaluations were carried out through a team-based approach, with the reviewer who scored mouse function blinded to treatment groups. Specifically, QC and DT were the surgeons responsible for performing MCAO surgeries. LH performed the random grouping. XG, QC and DT determined neurological scores and sliced and stained the brains. LH and XG calculated the infarct volumes. QC, DT and XG were blinded to the experimental design.

Statistical analysis

Data were collected in triplicate and reported as mean and standard deviation. Kaplan-Meier method was used to analyze the survival data. A log-rank test was used to determine the difference in survival between treatment groups. Comparison of the neurological score and infract area between two conditions was evaluated using the Kruskal-Wallis rank sum test. A p-value less than 0.05 was considered to be statistically significant.

Results

Design, synthesis and characterization of NPs

The schematic diagram of a typical PLGA-CTX/LEX NP was illustrated in Figure 1, *A*. NPs were synthesized through double emulsion procedures using PLL-conjugated PLGA as the starting material. The resulting NPs were modified with NHS-PEG-Mal to display PEG and maleimide functional groups. LEX was encapsulated in NPs during the emulsion with an entrapment efficiency of 33.8% and a loading efficiency of 0.8%. CTX was conjugated to the surface of NPs through the maleimide groups at a ratio of 800 molecules CTX per NP. Control NPs with modification of CTX alone, LEX alone or no modification were synthesized using the same procedures. PLGA-CTX/LEX NPs were spherical in

morphology (Figure 1, *B*). Encapsulation of IR780 or NEP1-40 did not change the size of NPs. The hydrodynamic radii of IR780-loaded PLGA-CTX/LEX NPs (Figure 1, *C*) and NEP1-40-loaded PLGA-CTX/LEX NPs (Figure 1, *D*) had no notable difference with values of 153.2 nm and 151.8 nm, respectively. All NPs had negative zeta potentials varying from −22.5 to −25.1 mV. Major components of NEP1-40-loaded PLGA- CTX/LEX NPs and their functions are illustrated in Figure 1, *E*.

Fluorescent imaging of NP delivery

We evaluated PLGA-CTX/LEX NPs for drug delivery to the ischemic microenvironment inside the brain in mice, which were established through MCAO surgery with 1-hour occlusion. The success of surgery was validated by cerebral blood flow measurement. Only those mice experienced >85% reduction of cerebral blood flow from baseline were included. PLGA NPs without modifications and PLGA NPs modified with CTX (PLGA-CTX NPs) or LEX (PLGA-LEX NPs) were used as controls. NPs were synthesized with encapsulation of IR780, a near-infrared fluorescence dye that allows for non-invasive detection in live animals. Twenty-four hours after intravenous injection, mice were subjected to imaging using an IVIS system. We found that among all groups, mice that received treatment of PLGA-CTX/LEX NPs had the highest fluorescence intensity and the fluorescence signal was specifically located ipsilaterally to the hemisphere of MCAO surgery, corresponding to the infarcted area (Figure 2, *A* and *B*). The average fluorescence intensity in mice treated with PLGA-CTX/LEX NPs was 1.6-fold, 2.5-fold, and 6.1-fold greater than those for mice treated with PLGA-LEX NPs, PLGA-CTX NPs and PLGA NPs, respectively (Figure 2, *C*). The differences among different groups were not due to surgical variances, as the cerebral blood flows across the groups were comparable (between 90-96%; Figure 2, *D*). The ratio of fluorescence intensity in the ischemic hemisphere to fluorescence intensity in the contralateral non-ischemic hemisphere was also analyzed. We found that the ratio was up to 5.5 fold in the group that received treatment of PLGA-CTX/LEX NPs (Figure 2, *C*). In contrast, the ratios for mice received treatments of PLGA NPs, PLGA-CTX NPs and PLGA-LEX NPs were 1.3, 1.9 and 5.1, respectively (Figure 2, *C*).

Autocatalysis as an efficient mechanism

According to our proposed autocatalytic mechanism, a fraction of NPs enter the ischemic microenvironment through CTX-mediated targeted delivery. The BBB modulator, LEX, is then released from the NPs and transiently enhances BBB permeability to allow more NPs to enter the same region. Therefore, through this autocatalytic mechanism, the delivery process creates a positive feedback loop. Consequently, the accumulation of NPs in the ischemic microenvironment inside the brain increases with subsequent administrations. To test this hypothesis, we pre-treated mice with unlabeled PLGA-CTX/LEX NPs for 0, 1, or 2 times before the final administration of IR780-loaded PLGA-CTX/LEX NPs and monitored the delivery efficiency based on fluoresce intensities in the ischemic hemisphere. In accordance with our proposed mechanism, we found that delivery autocatalytically increased with increased administrations (Figure 3, *A* and *B*). The fluorescence intensities in mice that received 1 and 2 pre-treatments were 1.9 and 3.5-fold greater than the intensity in mice that did not receive pre-treatment (Figure 3, *C*). For the group received two pre-treatments, mice were euthanized after the live imaging. The brains were isolated, sliced, and further imaged

to determine the location of NPs within the brain. We found that the fluorescence was primarily located in the ischemic hemisphere (Figure 3, *B*). The ratio of fluorescence intensity between the ipsilateral hemisphere and the contralateral hemisphere was calculated to be up to 12.8-fold (Figure 3, *C*). As a result, the fluorescence intensity in the ischemic region of the brain was comparable to that in the peripheral organs (Figure 3, *D*). We quantified the fluorescence intensities in major organs and found that the intensity in the brain was 25% and 77% of these in the liver and kidney, which had the highest values (Figure 3, *E*). These results suggest that PLGA-CTX/LEX NPs are capable of crossing the BBB and enrich in the ischemic microenvironment inside the brain with high efficiency.

In addition to the high efficiency, PLGA-CTX/LEX NPs also demonstrated a great specificity for the ischemic region. We sectioned the brains isolated from mice that received two pre-treatments with unlabeled PLGA-CTX/LEX NPs prior to treatment with IR780-loaded PLGA-CTX/LEX NPs. The brain slices were further subjected to TTC staining and imaging. Our results suggested that the location of ischemic tissue (white, TTC staining signal) overlapped with the location of NPs (red to yellow, IR780 signal, Figure 3, *F*). Fluorescence was also found in the penumbra region (the 4th sliced brain) that is located in the area surrounding of the ischemic core (Figure 3, *F*). The specificity of PLGA-CTX/LEX NPs is likely resulted from CTX, as PLGA-LEX NPs lacked such specificity (Figure 3, *G*). We noticed the signal in the brain from mice receiving treatments of PLGA-LEX NPs was not evenly distributed, with the signal in the middle of the brain slices greater than that on the right (Figure 3, G). Without the ligand CTX, PLGA-LEX NPs can only penetrate into the region with a compromised BBB. In this case, the efficiency of penetration depends on the degree of BBB compromise and the volume of blood flow. The probability of NP penetration correlates positively with blood flow. As suggested by TTC staining, the majority of tissue in the right brain was dead and thus had less blood flow than the region more centrally located. It is likely that this difference in blood flow is the reason for the variable distribution of NPs in the ischemic region.

PLGA-CTX/LEX NPs as a vehicle for stroke treatment

We next evaluated the use of PLGA-CTX/LEX NPs for ischemic stroke treatment by encapsulating peptide NEP1-40 as a model drug. Treatment with peptide NEP1-40 was recently reported to effectively improve neurological outcomes in ischemic rats.[33,34] Mice receiving successful MCAO surgeries were randomly grouped and received treatment with NEP1-40-loaded NPs, blank NPs, free NEP1-40, or saline for three times at 0, 24 and 48 hours after surgery. Mouse survival and behavior were monitored over 14 days. We found that systemic treatment of NEP1-40-loaded PLGA-CTX/LEX NPs markedly prolonged the survival of mice that had undergone MCAO surgery. The median survival time of the mice treated with the NEP1-40-loaded NPs was greater than 14 days (Figure 4, *A*), which was significantly longer than those for mice treated with saline (2.5 d; Figure 4, *A*, $p < 0.05$), free NEP1-40 (5 d; Figure 4, *A*, $p < 0.05$), blank NPs (2.5 d; Figure 4, *A*, $p < 0.05$), NEP1-40-loaded PLGA/LEX NPs (1 d; Figure S1), or NEP1-40-loaded PLGA-CTX NPs (3 d; Figure S1).

We measured the infarct volumes in mice with different treatments using standard TTC staining 3 days after MCAO (Figure 4, *B*). Consistent with the findings in survival, we found that systemic treatment with NEP1-40-loaded NPs significantly reduced the infarct sizes. The average percentage of infarct sizes in the NEP1-40-loaded NP treatment group was 20%, compared to 39% and 34% for mice treated with blank NPs and free NEP1-40, respectively.

The neurological outcomes of mice receiving different treatments were also assessed (Figure S2). We found that the treatment with NEP1-40-loaded NPs improved animals' neurological performance. For example, on post-operative day 3, 42% of mice receiving NEP1-40-loaded NPs displayed no neurological deficits, whereas only 8% of mice receiving blank NPs and 16% of mice receiving free NEP1-40-loaded NPs showed comparable neurological function (or no neurological deficits).

Taken together, our results suggest that PLGA-CTX/LEX NPs are a promising vehicle that can be employed for systemic delivery of therapeutic agents to the ischemic microenvironment inside the brain for stroke treatment.

Discussion

In the present study, we proposed an innovative approach for drug delivery to the ischemic microenvironment inside the brain through the combination of the traditional ligand-mediated approach, with a novel autocatalysis mechanism, which is designed to augment delivery efficiency. Our results demonstrated that, the resulting NPs synthesized based on this approach, PLGA-CTX/LEX NPs, efficiently crossed the BBB in the ischemic brain with high specificity. In contrast, NPs engineered either through the ligand-mediated mechanism alone or through the autocatalysis alone did not have a comparable efficiency (Figure 2), suggesting that either the targeted delivery approach or the autocatalysis is indispensable. This result is consistent with previous finding that traditional engineering approaches alone are insufficient to overcome the BBB.[19,21,22] Since MMP-2 is a secreted protein, the negative-charged PLGA-CTX/LEX NPs may stay in the ischemic microenvironment outside the damaged neurons after binding to MMP-2. The critical role of autocatalysis was also supported by the observation that the delivery efficiency of PLGA-CTX/LEX NPs exponentially increased with subsequent administrations (Figure 3).

We further demonstrated that because of their efficiency and specificity for the ischemic microenvironment inside the brain, PLGA-CTX/LEX NPs have a great potential to be employed as a vehicle for targeted delivery of therapeutics for stroke treatment. Intravenous administration of NEP1-40-loaded PLGA-CTX/LEX NPs significantly reduced infarct volumes, improved neurological function, and enhanced the survival of stroke mice. In contrast, treatment with free NEP1-40 at the same dose did not show a comparable therapeutic benefit (Figure 4). These results substantiated the fact that the degree of BBB disruption in the ischemic brain is unpredictable and insufficient for delivery of certain therapeutics to the brain in a pharmacologically significant quantity, and that the development of an efficient drug delivery system is critical for the improved treatment of ischemic stroke.

The combinatorial delivery approach tested in this study was achieved through the use of CTX and LEX. In the current literature, there are limited numbers of ligands that have been characterized for targeted drug delivery to the ischemic microenvironment inside the brain.[35,36] In this study, we demonstrated CTX as a promising ligand for targeted drug delivery to the ischemic microenvironment inside the brain. CTX-modified NPs specifically located in the ischemic regions (Figure 3, *F* and *G*), whereas unmodified NPs did not have such a specificity. However, CTX may not represent the best ligand for stroke delivery. It is worthwhile to explore additional ligands for further enhanced efficiency. Similarly, there are several BBB modulators other than LEX, such as 1-(6-amino-9H-purin-9-yl)-1-deoxy-N-ethyl-β-D-ribofuranuronamide (NECA),[27] labradimil,[37] and borneol,[38] those can be optimized for autocatalytic drug delivery to the ischemic microenvironment inside the brain.

The major components of the NPs developed in this study include PLGA, PEG, LEX and CTX. PLGA is a polymer that was approved by the FDA for clinical use in 1969 and since that time, has been in continuous, safe clinical use. PEG is classified by the FDA as "Generally Regarded as Safe" (GRAS) based on its long history of safety in humans[39]. LEX is a small molecule drug approved by the FDA for myocardial perfusion imaging[27,28]. CTX is a small peptide that has passed rigorous preclinical safety tests and entered a phase I clinical trials[40]. Therefore, it is likely that, compared to most other formulations previously reported[41], PLGA-CTX/LEX NPs reported in this study have a more favorable safety profile. We evaluated the interaction of PLGA-CTX/LEX NPs with erythrocytes and found they did not show detectable hemolysis effects at the tested doses (Figure S3). However, we cannot definitively exclude the possibility that PLGA-CTX/LEX NPs could generate immune response in human use. In the specific formulation described in this study, PEG was used a linker to conjugate CTX. There are conflicting reports in literature that PEG may elicit immune response through production of anti-PEG antibodies[42]. Future evaluation on the PEG-related immune response is warranted. If a significant immune response is observed, we may optimize the nanoparticles by replacing PEG with zwitterionic molecules, which have a more favorable immunogenicity profile but may retain similar stealth characteristics as PEG[43].

In conclusion, we have proposed and validated a novel combinational approach for systemic drug delivery to the ischemic microenvironment inside the brain. Based on this mechanism, we have developed PLGA-based NPs that provide targeted and efficient drug delivery to ischemic microenvironment inside the brain. The major components of PLGA-CTX/LEX NPs include PLGA, a biodegradable polymer that has been safely used in the clinic for over 40 years, and LEX, an FDA-approved small molecule drug with proven safety profile. Due to the high efficiency in crossing the BBB, targeting the ischemic stroke, and the construction from safe materials with minimal toxicity, PLGA-CTX/LEX NPs have the potential to serve as a new approach for the clinical management of stroke.

Supplementary Material

Refer to Web version on PubMed Central for supplementary material.

Acknowledgement

This work was supported by NIH Grants NS095817, NS095147, AHA grant 15GRNT25290018, and a Yale Center for Clinical Investigation CTSA Scholar Award (UL1 TR000142). QC, DT, XG and ZC were partially supported by scholarships from the Chinese Scholarship Council.

References

1. Go AS, Mozaffarian D, Roger VL, Benjamin EJ, Berry JD, Blaha MJ, et al. Heart disease and stroke statistics--2014 update: a report from the American Heart Association. Circulation. 2014; 129:e28. [PubMed: 24352519]
2. Kimberly WT, Battey TW, Pham L, Wu O, Yoo AJ, Furie KL, et al. Glyburide is associated with attenuated vasogenic edema in stroke patients. Neurocritical care. 2014; 20:193–201. [PubMed: 24072459]
3. Schwamm LH, Ali SF, Reeves MJ, Smith EE, Saver JL, Messe S, et al. Temporal trends in patient characteristics and treatment with intravenous thrombolysis among acute ischemic stroke patients at Get With The Guidelines-Stroke hospitals. Circulation. Cardiovascular quality and outcomes. 2013; 6:543–9. [PubMed: 24046398]
4. Yoo AJ, Verduzco LA, Schaefer PW, Hirsch JA, Rabinov JD, González RG. MRI-based selection for intra-arterial stroke therapy value of pretreatment diffusion-weighted imaging lesion volume in selecting patients with acute stroke who will benefit from early recanalization. Stroke. 2009; 40:2046–54. [PubMed: 19359641]
5. Šaňák D, Nosál V, Horák D, Bártková A, Zeleňák K, Herzig R, et al. Impact of diffusion-weighted MRI-measured initial cerebral infarction volume on clinical outcome in acute stroke patients with middle cerebral artery occlusion treated by thrombolysis. Neuroradiology. 2006; 48:632–9. [PubMed: 16941183]
6. Broderick JP, Palesch YY, Demchuk AM, Yeatts SD, Khatri P, Hill MD, et al. Endovascular therapy after intravenous t-PA versus t-PA alone for stroke. New England Journal of Medicine. 2013; 368:893–903. [PubMed: 23390923]
7. Mlynash M, Lansberg MG, De Silva DA, Lee J, Christensen S, Straka M, et al. Refining the definition of the malignant profile insights from the DEFUSE-EPITHET pooled data set. Stroke. 2011; 42:1270–5. [PubMed: 21474799]
8. Hacke W, Schwab S, Horn M, Spranger M, De Georgia M, von Kummer R. 'Malignant'middle cerebral artery territory infarction: clinical course and prognostic signs. Archives of neurology. 1996; 53:309–15. [PubMed: 8929152]
9. Rhim T, Lee DY, Lee M. Drug delivery systems for the treatment of ischemic stroke. Pharmaceutical research. 2013; 30:2429–44. [PubMed: 23307348]
10. Hu X, Zhang M, Leak RK, Gan Y, Li P, Gao Y, et al. Delivery of neurotherapeutics across the blood brain barrier in stroke. Curr Pharm Des. 2012; 18:3704–20. [PubMed: 22574984]
11. Kreuter J. Nanoparticulate systems for brain delivery of drugs. Adv Drug Deliv Rev. 2001; 47:65–81. [PubMed: 11251246]
12. Begley DJ. The blood-brain barrier: principles for targeting peptides and drugs to the central nervous system. J Pharm Pharmacol. 1996; 48:136–46. [PubMed: 8935161]
13. Latour LL, Kang DW, Ezzeddine MA, Chalela JA, Warach S. Early blood-brain barrier disruption in human focal brain ischemia. Annals of neurology. 2004; 56:468–77. [PubMed: 15389899]
14. Warach S, Latour LL. Evidence of reperfusion injury, exacerbated by thrombolytic therapy, in human focal brain ischemia using a novel imaging marker of early blood-brain barrier disruption. Stroke; a journal of cerebral circulation. 2004; 35:2659–61. [PubMed: 15472105]
15. Jiao H, Wang Z, Liu Y, Wang P, Xue Y. Specific role of tight junction proteins claudin-5, occludin, and ZO-1 of the blood-brain barrier in a focal cerebral ischemic insult. Journal of molecular neuroscience : MN. 2011; 44:130–9. [PubMed: 21318404]
16. Kuntz M, Mysiorek C, Petrault O, Petrault M, Uzbekov R, Bordet R, et al. Stroke-induced brain parenchymal injury drives blood-brain barrier early leakage kinetics: a combined in vivo/in vitro

study. Journal of cerebral blood flow and metabolism : official journal of the International Society of Cerebral Blood Flow and Metabolism. 2014; 34:95–107.

17. Kaplan B, Brint S, Tanabe J, Jacewicz M, Wang XJ, Pulsinelli W. Temporal thresholds for neocortical infarction in rats subjected to reversible focal cerebral ischemia. Stroke; a journal of cerebral circulation. 1991; 22:1032–9. [PubMed: 1866750]
18. Deeken JF, Loscher W. The blood-brain barrier and cancer: transporters, treatment, and Trojan horses. Clinical cancer research : an official journal of the American Association for Cancer Research. 2007; 13:1663–74. [PubMed: 17363519]
19. Patel T, Zhou J, Piepmeier JM, Saltzman WM. Polymeric nanoparticles for drug delivery to the central nervous system. Advanced drug delivery reviews. 2012; 64:701–5. [PubMed: 22210134]
20. Zhou J, Atsina KB, Himes BT, Strohbehn GW, Saltzman WM. Novel delivery strategies for glioblastoma. Cancer J. 2012; 18:89–99. [PubMed: 22290262]
21. Lanza GM, Marsh JN, Hu G, Scott MJ, Schmieder AH, Caruthers SD, et al. Rationale for a nanomedicine approach to thrombolytic therapy. Stroke; a journal of cerebral circulation. 2010; 41:S42–4. [PubMed: 20876503]
22. Thompson BJ, Ronaldson PT. Drug delivery to the ischemic brain. Adv Pharmacol. 2014; 71:165–202. [PubMed: 25307217]
23. Deshane J, Garner CC, Sontheimer H. Chlorotoxin inhibits glioma cell invasion via matrix metalloproteinase-2. J Biol Chem. 2003; 278:4135–44. [PubMed: 12454020]
24. Clark AW, Krekoski CA, Bou S-S, Chapman KR, Edwards DR. Increased gelatinase A (MMP-2) and gelatinase B (MMP-9) activities in human brain after focal ischemia. Neuroscience letters. 1997; 238:53–6. [PubMed: 9464653]
25. Chang DI, Hosomi N, Lucero J, Heo JH, Abumiya T, Mazar AP, et al. Activation systems for latent matrix metalloproteinase-2 are upregulated immediately after focal cerebral ischemia. Journal of cerebral blood flow and metabolism : official journal of the International Society of Cerebral Blood Flow and Metabolism. 2003; 23:1408–19.
26. Heo JH, Lucero J, Abumiya T, Koziol JA, Copeland BR, del Zoppo GJ. Matrix metalloproteinases increase very early during experimental focal cerebral ischemia. Journal of cerebral blood flow and metabolism : official journal of the International Society of Cerebral Blood Flow and Metabolism. 1999; 19:624–33.
27. Carman AJ, Mills JH, Krenz A, Kim DG, Bynoe MS. Adenosine receptor signaling modulates permeability of the blood-brain barrier. The Journal of neuroscience : the official journal of the Society for Neuroscience. 2011; 31:13272–80. [PubMed: 21917810]
28. Gao X, Qian J, Zheng S, Changyi Y, Zhang J, Ju S, et al. Overcoming the blood–brain barrier for delivering drugs into the brain by using adenosine receptor nanoagonist. ACS nano. 2014; 8:3678–89. [PubMed: 24673594]
29. Blum JS, Saltzman WM. High loading efficiency and tunable release of plasmid DNA encapsulated in submicron particles fabricated from PLGA conjugated with poly-L-lysine. Journal of Controlled Release. 2008; 129:66–72. [PubMed: 18511145]
30. Lavik EB, Hrkach JS, Lotan N, Nazarov R, Langer R. A simple synthetic route to the formation of a block copolymer of poly (lactic - co - glycolic acid) and polylysine for the fabrication of functionalized, degradable structures for biomedical applications. Journal of biomedical materials research. 2001; 58:291–4. [PubMed: 11319743]
31. Zhou J, Patel TR, Fu M, Bertram JP, Saltzman WM. Octa-functional PLGA nanoparticles for targeted and efficient siRNA delivery to tumors. Biomaterials. 2012; 33:583–91. [PubMed: 22014944]
32. Cai Q, Chen Z, Kong DK, Wang J, Xu Z, Liu B, et al. Novel microcatheter-based intracarotid delivery approach for MCAO/R mice. Neurosci Lett. 2015; 597:127–31. [PubMed: 25899778]
33. Wang F, Liang Z, Hou Q, Xing S, Ling L, He M, et al. Nogo-A is involved in secondary axonal degeneration of thalamus in hypertensive rats with focal cortical infarction. Neuroscience Letters. 2007; 417:6. [PubMed: 17383819]
34. Wang Q, Gou X, Xiong L, Jin W, Chen S, Hou L, et al. Trans-activator of transcription-mediated delivery of NEP1-40 protein into brain has a neuroprotective effect against focal cerebral ischemic

injury via inhibition of neuronal apoptosis. Anesthesiology. 2008; 108:1071–80. [PubMed: 18497608]

35. Lu, Y-m; Huang, J-y; Wang, H.; Lou, X-f; Liao, M-h; Hong, L-j, et al. Targeted therapy of brain ischaemia using Fas ligand antibody conjugated PEG-lipid nanoparticles. Biomaterials. 2014; 35:530–7. [PubMed: 24120040]
36. Hong H-Y, Choi JS, Kim YJ, Lee HY, Kwak W, Yoo J, et al. Detection of apoptosis in a rat model of focal cerebral ischemia using a homing peptide selected from in vivo phage display. Journal of Controlled Release. 2008; 131:167–72. [PubMed: 18692101]
37. Emerich DF, Dean RL, Osborn C, Bartus RT. The development of the bradykinin agonist labradimil as a means to increase the permeability of the blood-brain barrier - From concept to clinical evaluation. Clin Pharmacokinet. 2001; 40:105–23. [PubMed: 11286321]
38. Yu B, Ruan M, Dong X, Yu Y, Cheng H. The mechanism of the opening of the blood-brain barrier by borneol: a pharmacodynamics and pharmacokinetics combination study. Journal of ethnopharmacology. 2013; 150:1096–108. [PubMed: 24432371]
39. Suk JS, Xu Q, Kim N, Hanes J, Ensign LM. PEGylation as a strategy for improving nanoparticle-based drug and gene delivery. Advanced drug delivery reviews. 2015
40. Cheng Y, Zhao J, Qiao W, Chen K. Recent advances in diagnosis and treatment of gliomas using chlorotoxin-based bioconjugates. Am J Nucl Med Mol Imaging. 2014; 4:385–405. [PubMed: 25143859]
41. Kyle S, Saha S. Nanotechnology for the detection and therapy of stroke. Adv Healthc Mater. 2014; 3:1703–20. [PubMed: 24692428]
42. Schellekens H, Hennink WE, Brinks V. The immunogenicity of polyethylene glycol: facts and fiction. Pharmaceutical research. 2013; 30:1729–34. [PubMed: 23673554]
43. Amoozgar Z, Yeo Y. Recent advances in stealth coating of nanoparticle drug delivery systems. Wiley Interdiscip Rev Nanomed Nanobiotechnol. 2012; 4:219–33. [PubMed: 22231928]

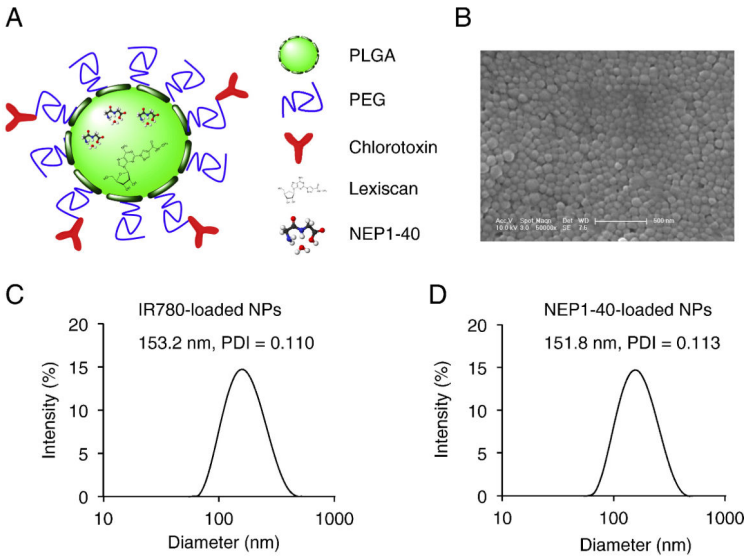

E

Component	Loading	Function
PLGA	92% (wt)	Drug protection and release control
PEG	9,600 per nanoparticle	Enhancing blood circulation
Lexiscan	0.8% (wt)	Enhancing BBB permeability
Chlorotoxin	800 per nanoparticle	Targeting MMP-2
NEP 1-40	1.1% (wt)	Neuroprotection

Figure 1.

Design and characterization of PLGA-CTX/LEX NPs. (**A**) Schematic diagram of a NEP1-40-loaded PLGA-CTX/LEX NP. (**B**) Representative image of NEP1-40-loaded PLGA-CTX/LEX NPs as captured by scanning electron microscope. Scale bar: 500 nm. Dynamic light scattering measurements of IR780-loaded PLGA-CTX/LEX NPs (**C**) and NEP1-40-loaded PLGA-CTX/LEX NPs (**D**). (**E**) Major components of PLGA-CTX/LEX NPs and their functions.

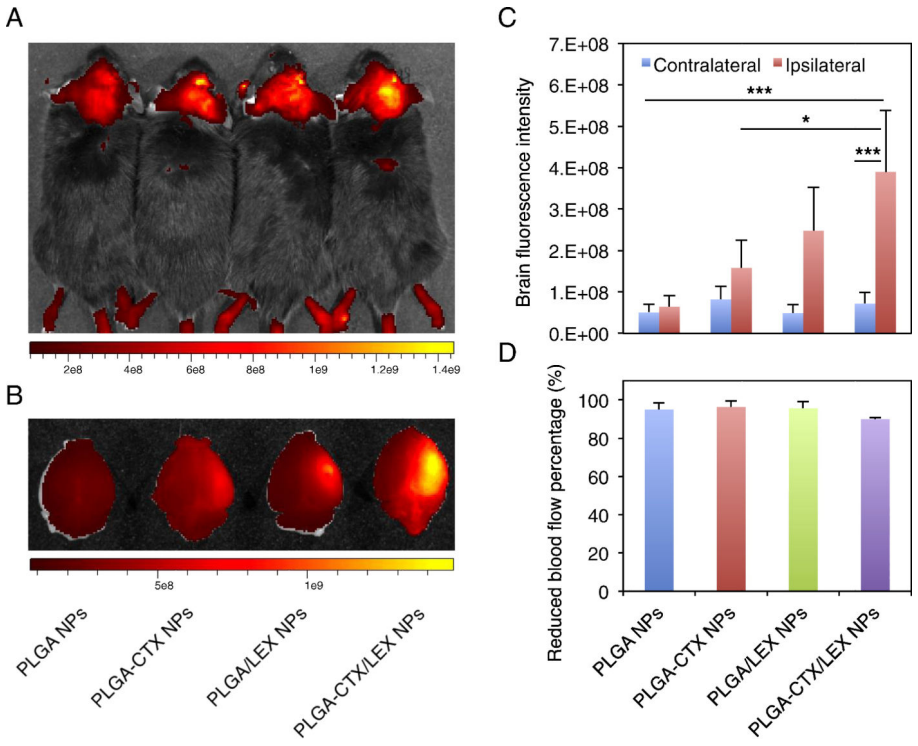

Figure 2.

Imaging of NPs in the ischemic brain. (**A**) Representative images of NPs in the brains of live animals. For each mouse, the head was shaved and the IR780 signal in the brain was acquired using an IVIS system 24 hours after intravenous administration of NPs (n = 3). (**B**) Representative images of NPs in the excised brains. (**C**) Semi-quantification of NPs in the excised brains. The intensity was quantified using Living Image 3.0. (**D**) Decrease of cerebral blood flow in mice before and during MCAO. All experiments were carried out in triplicate and the standard deviation is denoted using error bars. One-way ANOVA analysis was performed to determine the difference between groups. *$p < 0.05$. ***$p < 0.001$.

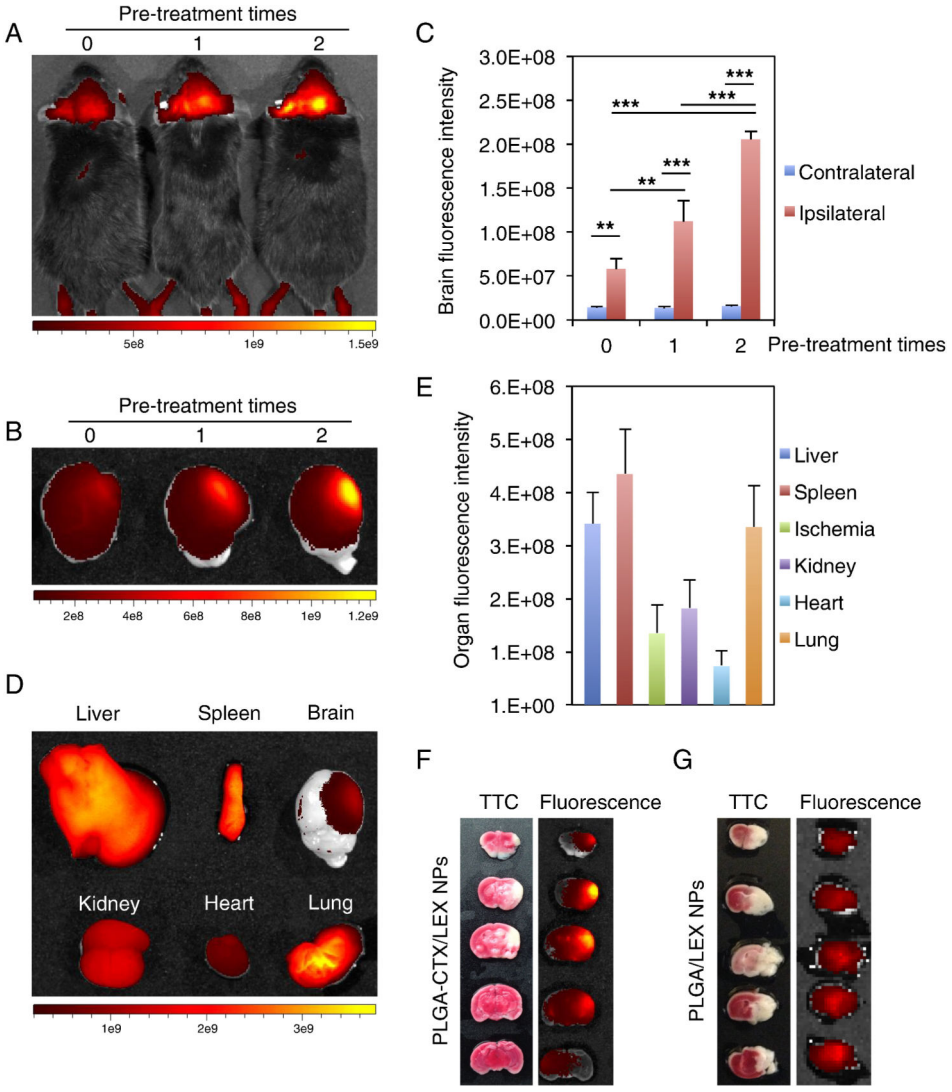

Figure 3.

Autocatalytic delivery of NPs to the ischemic brain. (**A-C**) The efficiency of PLGA-CTX/LEX NPs autocatalytically increased with subsequent administrations. Prior to the administration of IR780-loaded NPs, mice were pre-treated with saline or unlabeled PLGA-CTX/LEX NPs for indicated times (n = 3). Twenty-four hours later, fluorescence signals in live mice (**A**) and in the excised brains (**B**) were determined using an IVIS imaging system and the fluorescence intensities in the brain were quantified (**C**). Qualitative (**D**) and quantitative (**E**) imaging of NPs in major organs isolated from mice receiving 2 treatments of unlabeled PLGA-CTX/LEX NPs prior to the final administration of IR780-loaded PLGA-CTX/LEX NPs. All experiments were carried out in triplicate and the standard deviation is denoted using error bars. Images B and D were automatically processed by the IVIS imaging system by superimposing fluorescence images with white field images. The scale bars show fluorescence intensities but not white field signals. (**F**) Representative images of brain slices prepared from mice receiving 2 treatments of unlabeled PLGA-CTX/LEX NPs prior to the final administration of IR780-loaded PLGA-CTX/LEX NPs. The left panel represents TTC

staining and the right panel represents IR780 signal. (**G**) Representative images of brain slices prepared from mice receiving 2 treatments of unlabeled PLGA-LEX NPs prior to the final administration of IR780-loaded PLGA-LEX NPs. The left panel represents TTC staining and the right panel represents IR780 signal. One-way ANOVA analysis was performed to determine the differences between groups in Figure 3C. **P < 0.01. ***P < 0.001.

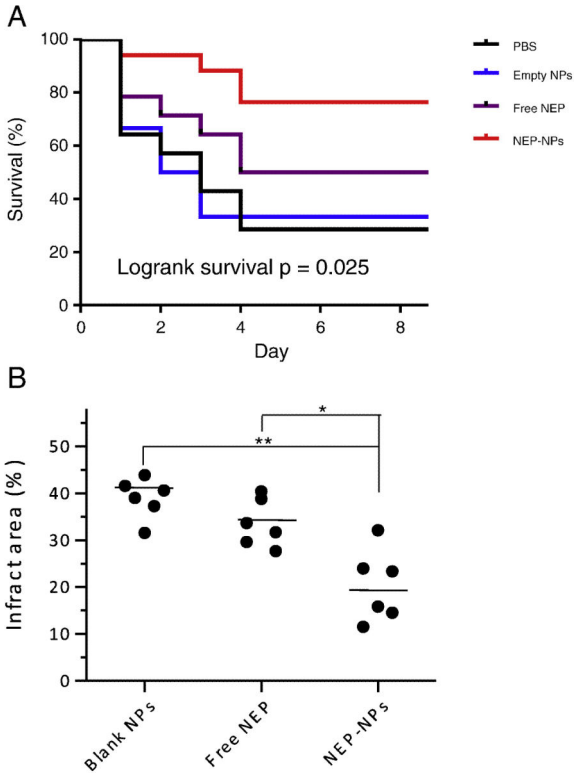

Figure 4.

Therapeutic evaluation of NEP1-40-loaded PLGA-CTX/LEX NPs. (**A**) Kaplan-Meier survival curves of MCAO mice receiving indicated treatments. Mice were treated with NEP1-40-loaded NPs (n = 17) three times at 0, 24 and 48 hours after surgery. Saline (n = 15), free NEP1-40 (n = 6), and blank NPs (n = 15) were used as controls. The dose of NEP1-40 was 22 μg per mouse for both the NEP1-40-loaded NP group and free NEP1-40 group (n = 10). Statistical analysis was performed using the Kaplan-Meier method. The differences among the four groups, between the group received NEP-NPs and the group received blank NPs, and between the group received NEP-NPs and the group received free NEP were calculated using the Kaplan-Meier method and found to be 0.025, 0.020 and 0.035, respectively. (**B**) Infarct volumes in mice receiving indicated treatments (n = 6). The ischemic region was identified by TTC staining and quantified by ImageJ (NIH). Comparison of the infract area between two conditions was evaluated by the Kruskal-Wallis rank sum test. *: $p < 0.05$; **: $p < 0.005$.